RAPID COMMUNICATIONS IN MASS SPECTROMETRY
Rapid Commun. Mass Spectrom. 2005; **19**: 2893–2904
Published online in Wiley InterScience (www.interscience.wiley.com). DOI: 10.1002/rcm.2139

RCM

Experimental and theoretical studies of the interaction of silver cluster cations Ag_n^+ (n = 1–4) with ethylene

Zhixin Tian*,† and Zichao Tang**

State Key Laboratory of Molecular Reaction Dynamics, Center of Molecular Science, Institute of Chemistry, Chinese Academy of Sciences, Beijing 100080, P.R. China

Received 28 July 2005; Revised 13 August 2005; Accepted 14 August 2005

Reactions of silver cluster cations Ag_n^+ with ethylene have been studied using a reflectron time-of-flight mass spectrometer. Chemisorbed $Ag_n(C_2H_4)_m^+$ (n = 1–3, m = 1–6) complexes were observed. For a given value of n, the abundances of $Ag_n(C_2H_4)_m^+$ (n = 1–3, m = 1–6) species first increase and then decrease, with the maximum of the intensity distribution usually at m = 4. This maximum does not change with the ethylene concentration in the mixed gas, the stagnation pressure of the mixed gas, or the size of Ag_n^+ (n = 1–3). A complementary extensive theoretical study on the structure and binding of $Ag_n(C_2H_4)_m^+$ (n = 1–4, m = 1–4) is also reported. Preferred binding sites, binding energies, geometries, vibrational frequencies, and ionization potentials are determined using density functional theory. Copyright © 2005 John Wiley & Sons, Ltd.

Transition metals and their derivatives, with their open electronic shells, complicated electronic structures, and several oxidation states, are among the most important catalysts in organometallic chemistry. This is mainly due to their activation of hydrocarbons (especially olefins) via donor–acceptor interactions[1–3] under the Dewar–Chatt–Duncanson model,[4,5] which has been widely used to describe the nature of the organometallic metal–olefin bond.

During the past several decades the complicated organometallic reaction mechanism has been investigated mainly by studying physical and chemical adsorption of ligand molecules on single crystal transition metal surfaces.[6–8] This situation was largely changed when Smalley and co-workers[9] published the laser vaporization method to produce bare metal clusters with a large variety of sizes and compositions. These metal clusters were soon proved to be an ideal bridge between atoms and bulk metals,[10,11] and can be taken as idealized models for metal surfaces. The reactivity of these clusters as a function of structure, size, composition, and charge can be studied conveniently.[12,13]

Some experimental techniques, such as near-edge X-ray absorption fine structure (NEXAFS) spectroscopy,[14] Raman spectroscopy,[15] and zero kinetic energy (ZEKE) spectroscopy,[16] have been used to obtain direct structural information on some metal clusters. Some new experimental[17] and theoretical techniques[18–20] or their combination have begun to provide some structural information about reactivity and size effects for large metal clusters.

Of the transition metals, silver is of particular interest for its catalytic epoxidation of olefins, especially ethylene, which is industrially important. In order to exploit the full potential of this reaction, it is important to first have a good picture of the interaction and mechanism between ethylene and the silver surface. The bi-directional interaction between the metal ion and olefin, described in the Dewar–Chatt–Duncanson model,[4,5] suggests a symmetric structure for the metal–olefin complex in which the metal ion is located symmetrically above the plane of the olefin molecule. The olefin acts as a σ-electron donor with the empty 5s atomic orbital of Ag^+ as the acceptor; on the other hand, the π^*-antibonding molecular orbital of the olefin also accepts electrons from the fully filled 4d shell of Ag^+, but the σ dative bond is the primary interaction.[21,22] The net result is that the C=C double bond in the olefin is weakened, i.e., activated.

Early in 1964, Hosoya and Nagakura[23] calculated the binding energy of the silver(1+)–ethylene complex. Later, Basch[21] studied the electronic structure of this complex using a non-empirical self-consistent field theory approach. Carter and Goddard[24] theoretically studied the adsorption of one ethylene molecule on Ag_3^+ and obtained five equilibrium isomers. The geometry of $Ag_2C_2H_4$ was optimized at the MP2 level.[25]

Infrared absorption spectra showed that a C_2H_4 molecule adsorbed on the Ag surface was deformed into a structure of C_{2V} symmetry;[26] four hydrogen atoms were pushed back to form a plane on the side of the C=C double bond opposite to that of Ag^+. This structure was similar to that in Zeise's salt ($KPtCl_3(C_2H_4).H_2O$)[27] or ethylene oxide.[28] However, electron energy loss spectroscopy (EELS)[29,30] and NEXAFS[31] spectra gave contradictory results, indicating that no substantial rehybridization occurred upon adsorption. In the reaction of silver clusters with ethylene studied by infrared

*Correspondence to: Z. Tian, Department of Chemistry, University of Minnesota, 207 Pleasant ST SE, Minneapolis, MN 55455, USA.
E-mail: tian@chem.umn.edu
**Correspondence to: Z. Tang, State Key Laboratory of Molecular Reaction Dynamics, Center of Molecular Science, Institute of Chemistry, Chinese Academy of Sciences, Beijing 100080, P.R. China.
E-mail: zctang@iccas.ac.cn
†Present address: Department Of Chemistry, University Of Minnesota, 207 Pleasant ST SE, Minneapolis, MN 55455, USA.
Contract/grant sponsor: National Natural Science Foundation of China; contract/grant number: 20203020.

photoionization coupled with time-of-flight mass spectrometry, Koretsky and Knickelbein[32] found that small silver clusters Ag_n (n = 3–7) adsorbed ethylene molecularly and the intensity of $Ag_n(C_2H_4)_m^+$ (n = 3–7, m = 1–3) complexes, obtained by photoionization at 193 nm ($h\nu = 6.42$ eV) of the corresponding neutrals, decreased quickly as m increased, such that $Ag_n(C_2H_4)_3^+$ could hardly be observed.

Although much effort has been expended on the structures of bare silver clusters and some individual silver–ethylene complexes, very few studies have been undertaken on the reactivity of small silver clusters as a function of size, on the nature of the binding of ethylene on bare silver clusters, and on the stabilities and structures of silver–ethylene complexes as a function of size and composition. Here we report extensive theoretical studies on the interaction of small silver cluster cations Ag_n^+ (n = 1–4) with ethylene molecules to form $Ag_n(C_2H_4)_m^+$ complexes. The theoretical results describe the nature of the binding of ethylene on silver cluster cations as a function of the size of the silver cluster and the number of ethylene molecules, and the equilibrium structures of $Ag_n(C_2H_4)_m^+$ (n = 1–4, m = 1–4) are obtained. Preferred binding sites, binding energies, geometries, vibrational frequencies, and ionization potentials are predicted using density functional theory (DFT). Most of the theoretical results are consistent with the corresponding experimental values.

EXPERIMENTAL

Reactions of silver cluster cations with ethylene were performed using a home-made reflectron time-of-flight mass spectrometer (RTOFMS) coupled with a laser vaporization source, which has been described in detail elsewhere;[33] only a brief description will be given here. The silver tablet is ablated by the focused second harmonic output of an Nd:YAG laser. The laser-vaporized metal plasma perpendicularly crosses the ethylene (seeded in Ar) supersonic beam and enters the 'growth channel', where formation of silver cluster cations and reactions of these cations with ethylene occur. The reaction products are cooled by supersonic expansion into vacuum through a conical nozzle. The expansion is carried by the pulsed argon through a conical skimmer and enters the pulsed extraction region of the RTOFMS. The product cations are extracted and detected in the RTOFMS. The final digitized TOF mass spectra are typically averaged over 1000 laser pulses to obtain better signal-to-noise ratios. The mass resolution of the mass spectrometer is about 1000 (FWHM) at $m/z = 1000$, as demonstrated previously.[33]

All materials and chemical reagents were obtained commercially and used as supplied without any further purification.

COMPUTATIONAL DETAILS

All calculations were performed at the DFT level using the B3LYP functional and GAUSSIAN 98 code.[34] A 6-311G(d, p) basis set with a single diffuse function was used for C and H and the effective core potential basis set LanL2DZ for Ag. The number of electrons and importance of electron correlation of transition-metal clusters make DFT a natural choice here.[35] Schwarz and co-workers[36] have conducted an extensive comparative computational study on the metal–ethylene complex, and concluded that B3LYP results showed remarkable agreement with the CCSD(T) data at a fraction of the computational effort. LanL2DZ has been proven reliable for silver-containing systems.[25,37–39] Kickelbick and Schubert[40] used the same level of theory and basis set as those adopted here to study $ClAgPH_3$ and $AgPH_3^+$, and the calculated structures were in very good agreement with crystallographic data.

Configurations of cationic and neutral $Ag_n(C_2H_4)_m$ were fully optimized under given symmetries, and stable equilibrium isomers for each $Ag_n(C_2H_4)_m^+$ complex were obtained. Frequency analysis was then performed to verify whether these isomers were local minima on potential energy surfaces (PESs) and to provide zero-point energies (ZPEs). ZPE correction was used with no scale factors. Population analysis was also performed to illustrate the binding nature of silver cluster cations with ethylene molecules.

In the calculation of adiabatic ionization potentials (AIPs), defined as the total energy difference between separately optimized cationic $Ag_n(C_2H_4)_m^+$ and the corresponding neutral species in the respective ground states, the optimization procedure described above and the initial configuration for the cationic $Ag_n(C_2H_4)_m^+$ were adopted for the corresponding neutral species. However, since Ag_3^+ assumes an equilateral triangular configuration with D_{3h} symmetry, while Ag_3 takes on an isosceles triangle configuration with C_{2v} symmetry[41,42] due to Jahn–Teller distortion, in the related calculation of neutral Ag_3 and its complexes with ethylene $Ag_3(C_2H_4)_m$ (m = 1–4), an isosceles triangle configuration was taken as the initial configuration in comparison with an equilateral shape for cationic Ag_3^+ and its complexes with ethylene $Ag_3(C_2H_4)_m^+$ (m = 1–4). This kind of problem obviously does not exist for Ag and Ag_2, while Ag_4 and Ag_4^+ have the same geometry (planar rhombus with D_{2h} symmetry[43,44]).

Single-point energy calculations of cationic $Ag_n(C_2H_4)_m^+$ complexes were performed at the geometries of the corresponding neutral complexes to determine the vertical ionization potentials (VIPs). A VIP is defined as the total energy difference between the ground state of the neutral and the corresponding cation at the same geometry as the neutral ground state.

Optimization of cationic and neutral Ag_n (n = 2–4), C_2H_4, and $Ag_nC_2H_4$ (n = 2–4) with all possible spin multiplicities was also performed to investigate the influence of multiplicity. The multiplicities with the lowest relative energy are adopted for the corresponding remaining neutral and cationic $Ag_n(C_2H_4)_m$ (n = 1–4, m = 2–4) complexes.

RESULTS

Experimental results

The reactions of silver cluster cations with supersonic ethylene seeded in argon were investigated with different ethylene concentrations and stagnation pressures. The predominant reaction channel observed under vaporization-expansion conditions was association of ethylene to form $Ag_n(C_2H_4)_m^+$ (n = 1–3, m = 1–6). These silver–ethylene complexes are chemisorbed species rather than physisorbed ones,

for the bonding of the physisorbed species was too weak to survive sufficiently long to reach the detector. TOF mass spectra of cationic products obtained from the reaction of silver cluster cations with supersonic ethylene, with five different ethylene concentrations and three different stagnation pressures, are shown in Figs. 1 and 2, respectively.

The association products $Ag_n(C_2H_4)_m^+$ are the dominant species observed in Figs. 1 and 2. The intensity distribution of $Ag_n(C_2H_4)_m^+$, for a given n value, shows first an increase and then a decrease as m increases. The nature of this distribution did not change with the size of the metal cluster Ag_n^+, the concentration of ethylene in the mixed gas, or the stagnation pressure of the mixed gas. In addition, the $Ag_n(C_2H_4)_m^+$ complexes tended to grow larger with higher ethylene concentrations; this was especially obvious in the intensity change of $Ag(C_2H_4)_5^+$ and $Ag(C_2H_4)_6^+$. Pure ethylene clusters $(C_2H_4)_m^+$ (m = 5–9), $Ag_nAr_k^+$ or $Ag_n(C_2H_4)_mAr_k^+$ with k ranging from 1–3 and m ranging from 1–5, also appear in Figs. 1 and 2; no detailed analysis of these species is presented here. As a summary of the experimental results, ethylene adsorbs as intact molecules on small silver cluster ions, and a stable solvent shell of ethylene seems to form at m = 4.

Theoretical studies

Relative energies of Ag_n and silver–ethylene complexes $Ag_nC_2H_4$ (including both neutral and cationic species, n = 2, 3, 4), with all possible multiplicities, are considered. Generally, the species with the smallest multiplicity are tens of kcal/mol lower in energy than those with other multiplicities, so the smallest multiplicities are adopted for all species here. The finally adopted multiplicities for cationic (neutral) $Ag_n(C_2H_4)_m$ (m = 0–4) are 1(2), 2(1), 1(2), 2(1), for

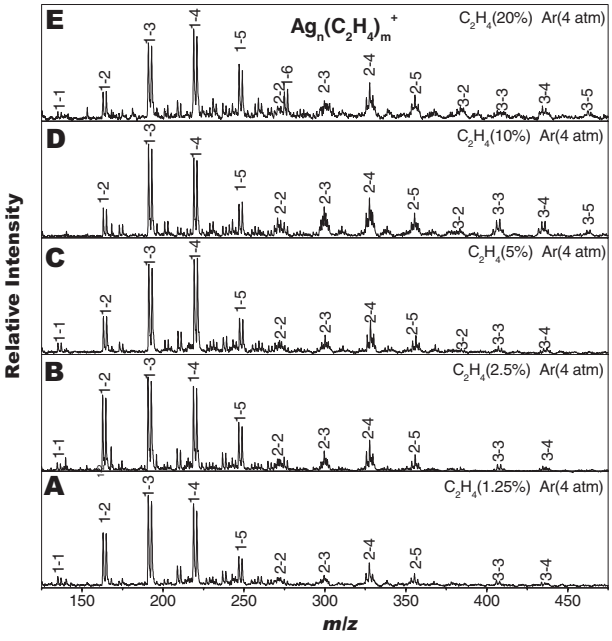

Figure 1. Typical TOF mass spectra for cationic products obtained from the Nd:YAG laser (532 nm, 10 mJ/pulse) irradiation of a silver tablet in the ethylene + Ar mixed carrier gas. The ethylene concentrations in the mixed gas are 1.25% (A), 2.50% (B), 5.00% (C), 10.00% (D), and 20.00% (E), respectively.

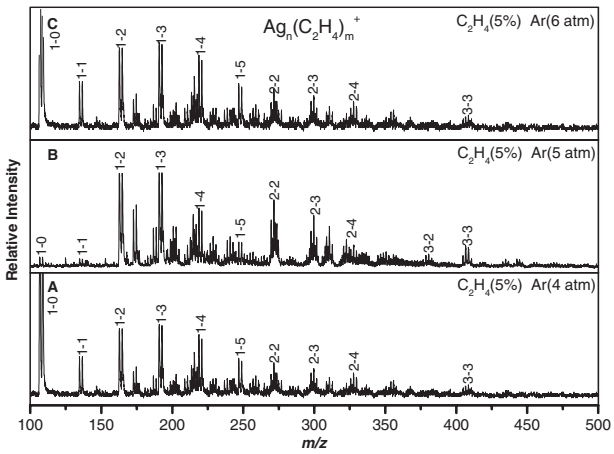

Figure 2. Typical TOF mass spectra for cationic products obtained from the Nd:YAG laser (532 nm, 10 mJ/pulse) irradiation of a silver tablet in the ethylene + Ar (95%) mixed carrier gas. The stagnation pressures of the mixed gas are 4 atm (A), 5 atm (B), and 6 atm (C), respectively.

n = 1, 2, 3, 4, respectively. Electron spin resonance (ESR) spectra of Ag_3 established the spin multiplicity S = ½,[41] which is consistent with our calculated results here. These multiplicities are those expected for the isolated Ag_n, Ag_n^+ clusters and have been previously established by many investigations.

The optimized spatial and electronic symmetries, equilibrium structures, and Mulliken atomic charges, for the most stable equilibrium isomer of Ag_n^+ (n = 2–4) and C_2H_4, are shown in Fig. 3. The optimized equilibrium structures and Mulliken atomic charges for the most stable equilibrium isomers of $Ag_n(C_2H_4)_m^+$ (n = 1–4, m = 1–4) are shown in Fig. 4. The silver cluster moiety in the most stable $Ag_n(C_2H_4)_m^+$ isomers all prefer to lie right above the ethylene molecule plane, in contrast with the parallel[45,46] or near-parallel[47] adsorption of the ethylene molecule on the silver surface in the condensed phase. Spatial and electronic symmetries, relative energies E_{rel}, ZPE-corrected binding energies D_0, and stretching vibration frequencies of the C=C double bond in the optimized stable equilibrium isomers of $Ag_n(C_2H_4)_m^+$, are shown in Table 1. E_{rel} is defined as the total energy difference between other equilibrium isomers and the most stable one, whose relative energy is set as zero. For the most stable $Ag_n(C_2H_4)_m$ isomers, VIPs and AIPs of the neutral species are also listed in the last two columns of Table 1. The optimized equilibrium configurations for stable isomers of $Ag_n(C_2H_4)_m^+$ (n = 1–4, m = 1–4), other than the most stable ones, are shown in Fig. 5.

All the optimized structures listed in Figs. 3, 4, and 5 were characterized by harmonic frequency analysis as local minima (all frequencies real).

$$Ag_n^+ (n = 2,\ 3,\ 4) \text{ and } C_2H_4$$

The calculated VIPs of Ag and Ag_2 are 7.75 and 7.80 eV, in good agreement with the experimental values of 7.57624 and 7.6557 eV, respectively.[48,49] The predicted AIP of Ag_3 is 5.69 eV. It is well known that the global minimum on the potential energy surface of the cationic Ag_4^+ cluster and the corresponding neutral species[50,51] assume the same D_{2h}

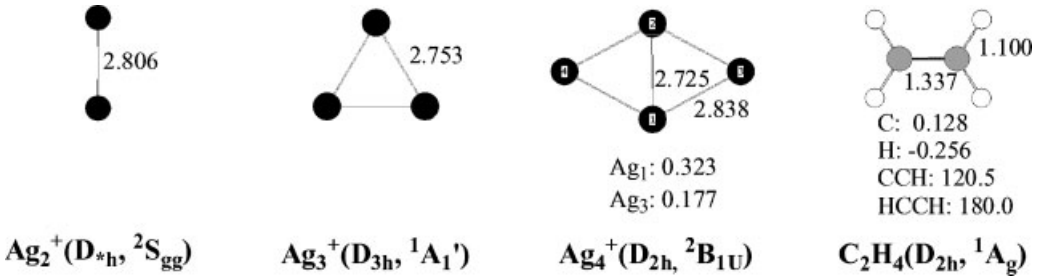

Figure 3. The optimized spatial and electronic symmetries, equilibrium structures, and Mulliken atomic charges for the most stable equilibrium isomer of the Ag_n^+ (n = 2–4) cluster and the C_2H_4 molecule. The bond lengths are in Å; the bond angles and the dihedral angles are in degrees.

rhombus equilibrium geometry (see Fig. 3), which leads to very close VIP (6.43 eV) and AIP (6.42 eV) values for the neutral Ag_4 cluster as calculated here. The calculated VIP of Ag_4 lies within the range of experimental values, 6.65 eV[52] and 6.3 eV,[53] obtained by electron impact ionization.

The free ethylene molecule is planar with D_{2h} symmetry, with a C=C double bond length of 1.337 Å, C–H bond lengths of 1.100 Å, and H–C–H angles of 119.0°, as shown in Fig. 3. These structural parameters are very close to the corresponding values obtained by high-level *ab initio* calculations (1.3307 Å, 1.0809 Å, and 121.47°).[54] The VIP of C_2H_4 calculated here is 10.59 eV, in good agreement with the experimental value of 10.51 eV obtained by chemi-ionization.[55] All the optimized structural parameters obtained here are much better than the latest results obtained using a double zeta basis set.[42]

$Ag(C_2H_4)_m^+$ (m = 1–4)

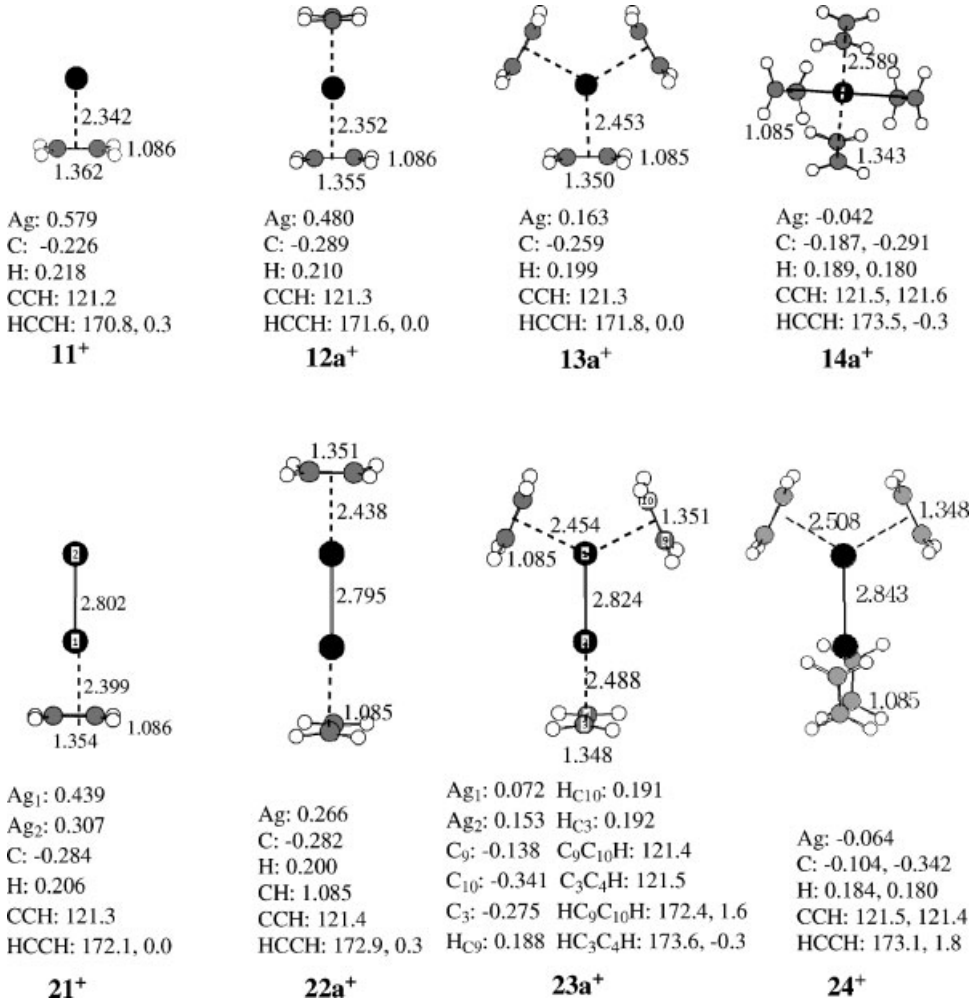

Figure 4. The optimized equilibrium structures and Mulliken atomic charges for the most stable equilibrium isomer of $Ag_n(C_2H_4)_m^+$ (n = 1–4, m = 1–4). Here a simple notation nmx$^+$ is used to represent $Ag_n(C_2H_4)_m^+$; n is the number of silver atoms, m is the number of ethylene molecules, x represents the xth isomer in increasing energy order for given n and m values. The bond lengths are in Å; the bond angles and the dihedral angles are in degrees.

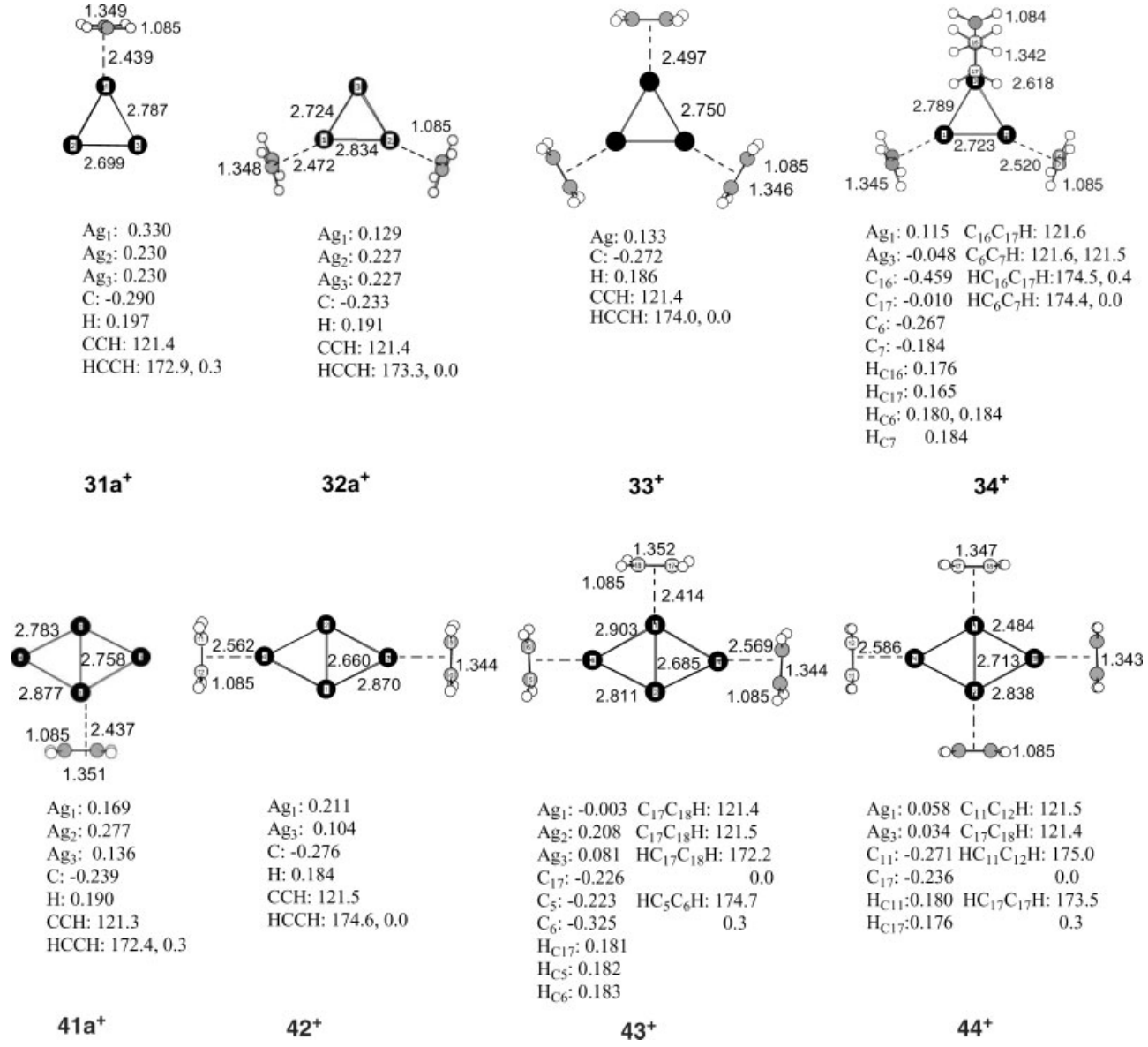

Figure 4. Continued

For $AgC_2H_4^+$, the Ag atom prefers to lie right above the ethylene molecule plane with C_{2v} symmetry, rather than within the ethylene molecular plane (Fig. 4, structure 11^+). The H atoms are tilted out of the original plane away from the complex by 4.6°. Ethylene here in its silver complex deforms from a D_{2h} local symmetry in the free ethylene molecule to a local C_{2v} symmetry. The calculated binding energy D_e of $AgC_2H_4^+$ is 31.6 kcal/mol (Table 1), close to a recent experimental value of 33.7 kcal/mol.[56]

Two equilibrium isomers that differ in the relative orientations of the C_2H_4 moieties in the linear C_2H_4–Ag^+–C_2H_4 structure (Fig. 4, structure $12a^+$ and Fig. 5, structure $12b^+$) are degenerate in energy (see Table 1), so the ground states of this pair of isomers should have essentially no barrier for ethylene molecules to rotate around the Ag–C_2H_4 central axis. This phenomenon was also observed in structures $13a^+$, $31a^+$, and $32a^+$, as discussed below. In $12a^+$, the Ag–ethylene molecule distance (defined as the vertical distance between the Ag atom and the ethylene molecule plane) (2.352 Å) is a little longer than that of $AgC_2H_4^+$ (2.342 Å), while the C=C double bond length (1.355 Å) is a little shorter than that of $AgC_2H_4^+$ (1.362 Å). These changes indicate a weaker binding between the Ag atom and the ethylene molecules due to the addition of the second ethylene molecule in $12a^+$. This tendency is also clear in the binding energies; the binding energy of $Ag(C_2H_4)_2^+$ (58.0 kcal/mol) is a little smaller than twice that of $AgC_2H_4^+$ (31.6 kcal/mol).

Two isomers of $Ag(C_2H_4)_3^+$ were found. The isomer with all ethylene molecules lying head-to-head has lower energy (Fig. 4, structure $13a^+$, and Table 1). The structural arrangement of the three ethylene molecules in $13a^+$ is analogous to that of tri[bicyclo[2.2.1]heptene]nickel(0) obtained by X-ray diffraction (XRD) experiments.[57] The silver–ethylene molecule distance in $13a^+$ (2.453 Å) is much longer than that of 11^+ (2.342 Å), and the binding energy of $13a^+$ (67.6 kcal/mol) is much lower than thrice that of 11^+ (31.6 kcal/mol). These data suggest that the addition of the third ethylene molecule significantly weakens the interaction between the Ag atom and the ethylene

RCM

Table 1. Spatial and electronic symmetries, relative energies E_{rel} (kcal/mol), ZPE-corrected binding energies D_0 (kcal/mol), and C=C double bond stretching vibration frequencies (cm^{-1}), of the optimized equilibrium isomers of $Ag_n(C_2H_4)_m^+$ (nmx^+) (n = 1–4, m = 1–4). VIPs and AIPs (eV) of corresponding neutral $Ag_n(C_2H_4)_m$ (nmx) (n = 1–4, m = 1–4) species are also listed in the last two columns

					nmx	
nmx^+	Sym	E_{rel}	D_0	C=C frequencies	VIP(exp*)	AIP
11^+	$C_{2V}/^1A_1$	/	31.6	1606.7	7.16	6.36
$12a^+$	$D_{2d}/^1A_1$	0.0	58.0	1620.3, 1623.3	7.10	5.15
$12b^+$	$D_{2h}/^1A_g$	0.2	57.9	/	/	/
$13a^+$	$D_{3h}/^1A_1$	0.0	67.6	1629.5, 1629.5, 1633.0	7.05	4.68
$13b^+$	$C_{2V}/^1A_1$	0.8	67.0	/	/	/
$14a^+$	$D_{2d}/^1A_1$	0.0	71.3	1645.1, 1645.3, 1645.3, 1648.7	7.05	4.49
$14b^+$	$C_1/^1A$	0.0	71.4	/	/	/
21^+	$C_{2V}/^2A_1$	0.0	21.5	1622.0	7.10	6.96
$22a^+$	$D_{2d}/^2A_1$	0.0	37.9	1628.3, 1629.6	6.55	6.30
$22b^+$	$D_{2h}/^2A_g$	0.0	38.0	/	/	/
$23a^+$	$C_{2V}/^2A_1$	0.0	46.2	1620.9, 1623.2, 1635.4	6.39	5.87
$23b^+$	$C_{2V}/^2A_1$	0.0	46.2	/	/	/
24^+	$D_{2d}/^2A_1$	0.0	51.3	1627.5, 1627.5, 1628.8, 1629.1	6.29	5.56
$31a^+$	$C_{2V}/^1A_1$	0.0	17.1	1633.3	5.43(5.4–5.2)	5.28
$31b^+$	$C_{2V}/^1A_1$	0.3	16.9	/	/	/
$32a^+$	$C_{2V}/^1A_1$	0.0	31.5	1635.9, 1636.7	5.01(5.2–4.9)	4.75
$32b^+$	$C_{2V}/^1A_1$	0.3	31.2	/	/	/
33^+	$D_{3h}/^1A_{1'}$	0.0	43.1	1640.6, 1640.6, 1642.0	5.05(5.2–4.9)	4.34
34^+	$C_{2V}/^1A_1$	0.0	45.1	1642.4, 1643.3, 1645.5, 1646.5	5.08	3.99
$41a^+$	$C_{2V}/^2B_2$	0.0	14.1	1627.7	6.23(6.4–6.0)	6.20
$41b^+$	$C_{2V}/^2A_1$	3.2	11.2	/	/	/
42^+	$D_{2h}/^2B_{3u}$	0.0	21.7	1642.7, 1643.7	5.98(6.4–6.0)	5.42
43^+	$C_{2V}/^2B_2$	0.0	34.7	1619.7, 1644.2, 1645.1	5.81(5.8–5.6)	5.36
44^+	$D_{2h}/^2B_{3u}$	0.0	44.0	1630.8, 1632.6, 1646.5, 1647.3	7.58	5.19

*Experimental VIPs are taken from Carter and Goddard.[24]

molecules, and that the effect of steric hindrance begins to appear.

As an effect of steric hindrance, the favorite configuration of $Ag(C_2H_4)_4^+$ is unlike that of $Ag(C_2H_4)_3^+$; two head-to-head ethylene molecules form a cross with the other two head-to-head ethylene molecules (see structure $14a^+$ in Fig. 4). In $14a^+$, the silver–ethylene molecule distance has increased significantly compared to $13a^+$ (from 2.453 Å to 2.589 Å), while the C=C double bond length (1.343 Å) is only slightly longer than that of the free ethylene molecule (1.337 Å). Obviously, there is a very weak interaction between the Ag atom and the ethylene molecules in $Ag(C_2H_4)_4^+$. The isomer with four ethylene molecules lying symmetrically on the four corners of a tetrahedron and the Ag atom at the center of the tetrahedron ($14b^+$ in Fig. 5) is degenerate in energy with $14a^+$.

$$Ag_2(C_2H_4)_m^+ \ (m = 1–4)$$

In the most stable equilibrium isomer of $Ag_2C_2H_4^+$, two Ag atoms lie on one side of the ethylene molecule, rather than the sandwich structure (M–ethylene–M^+) analogous to those found for $Ni_2C_2H_4$[58] and $Ag_2(C_6H_6)^+$ in photodissociation experiments.[59] Structure 21^+ has a much looser ion–molecule interaction between the silver moiety and the ethylene molecule. Compared with structure 11^+ for $AgC_2H_4^+$, the Ag atom lies further away from the ethylene molecule and the C=C double bond has much less increase in length. Sharing the positive charge with the second Ag atom is disadvantageous for the charge transfer between the positive ion and the ligand molecule and weakens the ion–molecule interaction.

The most stable equilibrium isomer of $Ag_2(C_2H_4)_2^+$ complexes is a symmetric molecule–ion–molecule sandwich structure ($22a^+$ in Fig. 4). Compared with 21^+, the addition of the second ethylene molecule in $22a^+$ does not bring much change in structure parameters of the whole complex. This suggests that two ethylene molecules interact with the two Ag atoms separately, and efficient ion–molecule interaction only exists between the adjacent atomic metal ion and ligand molecule. This kind of relationship between structures 21^+ and $22a^+$ also exists between $31a^+$ and $32a^+$, as discussed in the following section.

$$Ag_3(C_2H_4)_m^+ \ (m = 1–4)$$

In the energy-optimized equilibrium isomer of $Ag_3(C_2H_4)^+$ (structure $31a^+$ in Fig. 4), the Ag_3 moiety assumes an equilateral triangle geometry. This structure is about 10 kcal/mol lower in energy than that with the Ag_3 moiety assuming a right-angled triangle geometry, as shown by Carter and Goddard.[24] The Ag_3 moiety in structures $31a^+$ and $32a^+$ converges to an isosceles triangle configuration in comparison with the equilateral triangle configuration of the bare Ag_3^+ cluster, as a consequence of charge transfer from the ethylene molecules to the Ag_3 moiety. The net charge transfer from the ethylene molecules to the Ag_3 moiety and the binding energy are rather smaller than thrice the corresponding values for structure $31a^+$. The addition of the third ethylene molecule to the Ag_3^+ cluster significantly weakens the interaction, and this implies that the effects of steric hindrance begin to appear in 33^+.

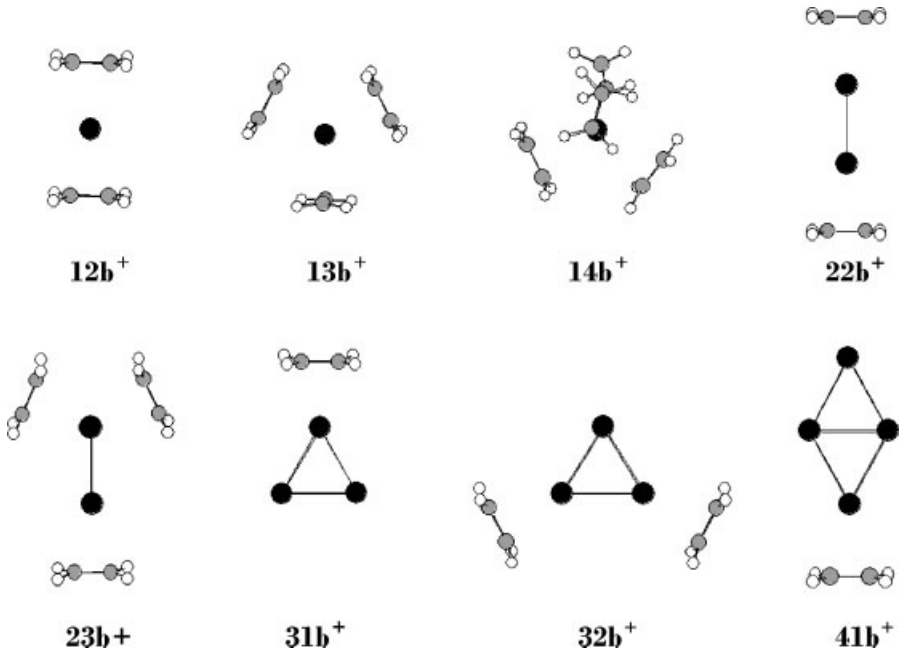

Figure 5. The optimized equilibrium geometries for the stable isomers of $Ag_n(C_2H_4)_m^+$ (n = 1–4, m = 1–4) other than the most stable ones shown in Fig. 4. The notation nmx^+ is the same as that used in Fig. 4.

$$Ag_4(C_2H_4)_m^+ \ (m = 1\text{–}4)$$

Among the equilibrium structures of $Ag_4C_2H_4^+$ complexes, the isomer with ethylene binding atop at the short diagonal position of the rhombic Ag_4 moiety (structure $41a^+$ in Fig. 4) is 2.9 kcal/mol lower in energy than the isomer with ethylene binding atop the long diagonal position (structure $41b^+$ in Fig. 5). This relationship also exists for the binding between the Ag_4 cluster and ammonia.[60]

Two ethylene molecules lie symmetrically above the two Ag atoms along the long diagonal of the rhombic Ag_4 moiety to form the most stable equilibrium isomer of the $Ag_4(C_2H_4)_2^+$ complex (structure 42^+ in Fig. 4). The addition of the second ethylene molecule weakens the binding between the Ag_4 moiety and the ethylene molecules in 42^+ compared with that in $41a^+$, as indicated by the silver–ethylene molecule distance (2.491 Å) that is larger than that in $41a^+$ (2.437 Å); also the net charge transfer from the ethylene molecules to the Ag_4 moiety (0.514) is much smaller than double that in $41a^+$ (0.282).

The ethylene molecules in the most stable equilibrium isomer of the $Ag_4(C_2H_4)_4^+$ complex (structure 44^+ in Fig. 4) lie head-to-head around the rhombic Ag_4 moiety like those in $13a^+$ and 33^+. The silver–ethylene molecule distance along the short diagonal of the rhombic Ag_4 moiety (2.484 Å) is far shorter than that along the long diagonal (2.672 Å); the C=C double bond length of the ethylene molecules lying along the short diagonal is a little longer than that along the long diagonal. Stronger binding of the metal cluster with the ligand molecules along the short diagonal is obvious.

DISCUSSION

Bond lengths and bond distances

The Ag–Ag bond length in $Ag_2(C_2H_4)_m^+$ (m = 1–4) seems to increase with increasing m; as m increases from 1 to 4, the Ag–Ag bond length increases from 2.802 to 2.846 Å, although the Ag–Ag bond length in structure $22a^+$ is slightly shorter than in 21^+. The increase in the average Ag–Ag bond length in $Ag_3(C_2H_4)_m^+$ (m = 1–4) is much more smooth than that in $Ag_2(C_2H_4)_m^+$ (m = 1–4), although $Ag_3(C_2H_4)_3^+$ seems to be special as its Ag–Ag bond length is the same as that in the bare Ag_3^+ cluster. For $Ag_4(C_2H_4)_m^+$ (m = 1–4), the addition of ethylene molecules along the short diagonal of the rhombic Ag_4 moiety increases the Ag–Ag bond length along the short diagonal; in the same way, the addition of ethylene molecules along the long diagonal increases the four Ag–Ag bond lengths along the sides of the rhombus.

Under the Dewar–Chatt–Duncanson model,[4,5] no matter whether the ethylene molecule acts a σ-electron donor or π-electron acceptor via the π^*-antibonding orbital, the C=C double bond is weakened, so the C=C double bond length is always elongated in ethylene bound with cationic silver clusters. This tendency is uniformly observed here for all $Ag_n(C_2H_4)_m^+$ (n = 1–4, m = 1–4) complexes. A summary of the elongation of the C=C double bond of ethylene in $Ag_n(C_2H_4)_m^+$ (n = 1–4, m = 1–4) with the variation of m is shown in Fig. 6(A); when several values of the C=C double bond length exist in the same $Ag_n(C_2H_4)_m^+$ complex for given n and m, the average value was adopted for this figure.

Some characteristics of Fig. 6(A) are now discussed. First, the elongation of the C=C double bond in the $Ag(C_2H_4)_m^+$ (m = 1–4) complexes rapidly decreases when m increases from 1 to 4, indicating that the binding of additional ethylene molecules strongly weakens the binding between the silver moiety and the original ethylene molecule(s). The binding between the larger silver moieties and the original ethylene molecule(s) in $Ag_n(C_2H_4)_m^+$ (n = 2–4, m = 1–4) seems to be less influenced by the addition of another ethylene molecule, since the net elongation of the C=C double bond in these

RCM

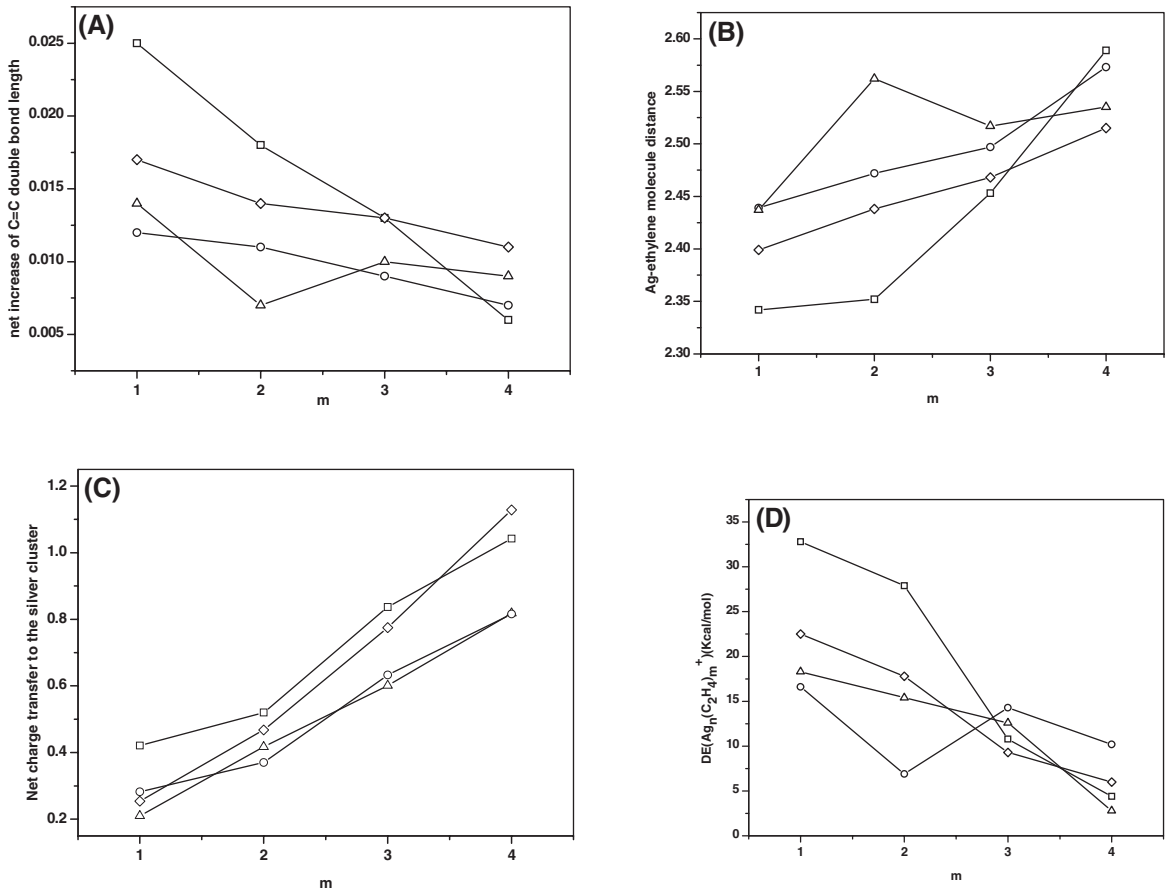

Figure 6. Increase of C=C double bond lengths (in Å) compared with that of the free ethylene molecule (A), the Ag–ethylene molecule distances (B), net Mulliken charge transfer from ethylene molecule(s) to silver cluster moiety (C), and binding energy change ($\Delta E(Ag_n(C_2H_4)_m^+)$) with the addition of another ethylene molecule (D) in the optimized most stable equilibrium isomers of $Ag_n(C_2H_4)_m^+$ (n = 1–4, m = 1–4). If several values appear in one complex at the same time, average values are adopted. □, ◇, ○, and Δ represent $Ag(C_2H_4)_m^+$, $Ag_2(C_2H_4)_m^+$, $Ag_3(C_2H_4)_m^+$, and $Ag_4(C_2H_4)_m^+$ (m = 1–4), respectively.

complexes shows a very slow decrease when m increases from 1 to 4, which indicates that only the adjacent Ag atom and ethylene molecule have an effective interaction. Second, for a given value of m, the net elongation of the C=C double bond in the $Ag_n(C_2H_4)^+$ (n = 1–4) species also shows a rapid decrease when n increases from 1 to 4, although this tendency is less marked when m increases from 1 to 4. The underlying interpretation for this phenomenon is that the distribution of the positive charge when the metal cluster grows larger is disadvantageous for the charge transfer between the metal cluster and the ligand molecule, which will be further discussed below.

The Ag–ethylene molecule distances in $Ag_n(C_2H_4)_m^+$ (n = 1–4, m = 1–4) with the variation of m are drawn in Fig. 6(B). When several values of the Ag–ethylene molecule distances exist in the same $Ag_n(C_2H_4)_m^+$ complex for given n and m, the average value was adopted. Except for a steep increase at m = 3 and 4 for $Ag(C_2H_4)_m^+$ (m = 1–4), the Ag–ethylene molecule distances in the remaining $Ag_n(C_2H_4)_m^+$ (n = 2–4, m = 1–4) species show a rather smooth increase when m increases from 1 to 4, in contrast with the decrease of the corresponding net elongation of the C=C double bonds.

Net charge transfer

The nature of the binding between the silver cluster moiety and ethylene in $Ag_n(C_2H_4)_m^+$ (n = 1–4, m = 1–4) can be demonstrated using the Mulliken atomic charge distribution and transfer. Here the $Ag_n(C_2H_4)_m^+$ (n = 1–4, m = 1–4) complexes are presumed to form from the silver cluster cations as a whole and individual ethylene molecules. The net charge transfer from the ethylene molecule(s) to the silver cluster moiety in $Ag_n(C_2H_4)_m^+$ (n = 1–4, m = 1–4) as a function of m is shown in Fig. 6(C).

The net charge transfer in $Ag_2(C_2H_4)_m^+$ (m = 1–4) increases more rapidly when m increases from 1 to 4 than for the remaining complexes $Ag_n(C_2H_4)_m^+$ (n = 1, 3, 4, m = 1–4), all of which have similar charge transfer curves. The net charge transfer in $Ag_n(C_2H_4)_m^+$ (n = 1–4, m = 1–4) ranges from the minimum of 0.21 for $Ag_3C_2H_4^+$ to the maximum of 1.128 for $Ag_2(C_2H_4)_4^+$; these rather large charge transfers between the silver cluster moiety and ethylene molecules indicate a coordination linkage.

Harmonic frequencies

Absolute frequency values corresponding to the no-barrier rotation around the Ag–C_2H_4 central axis of ethylene

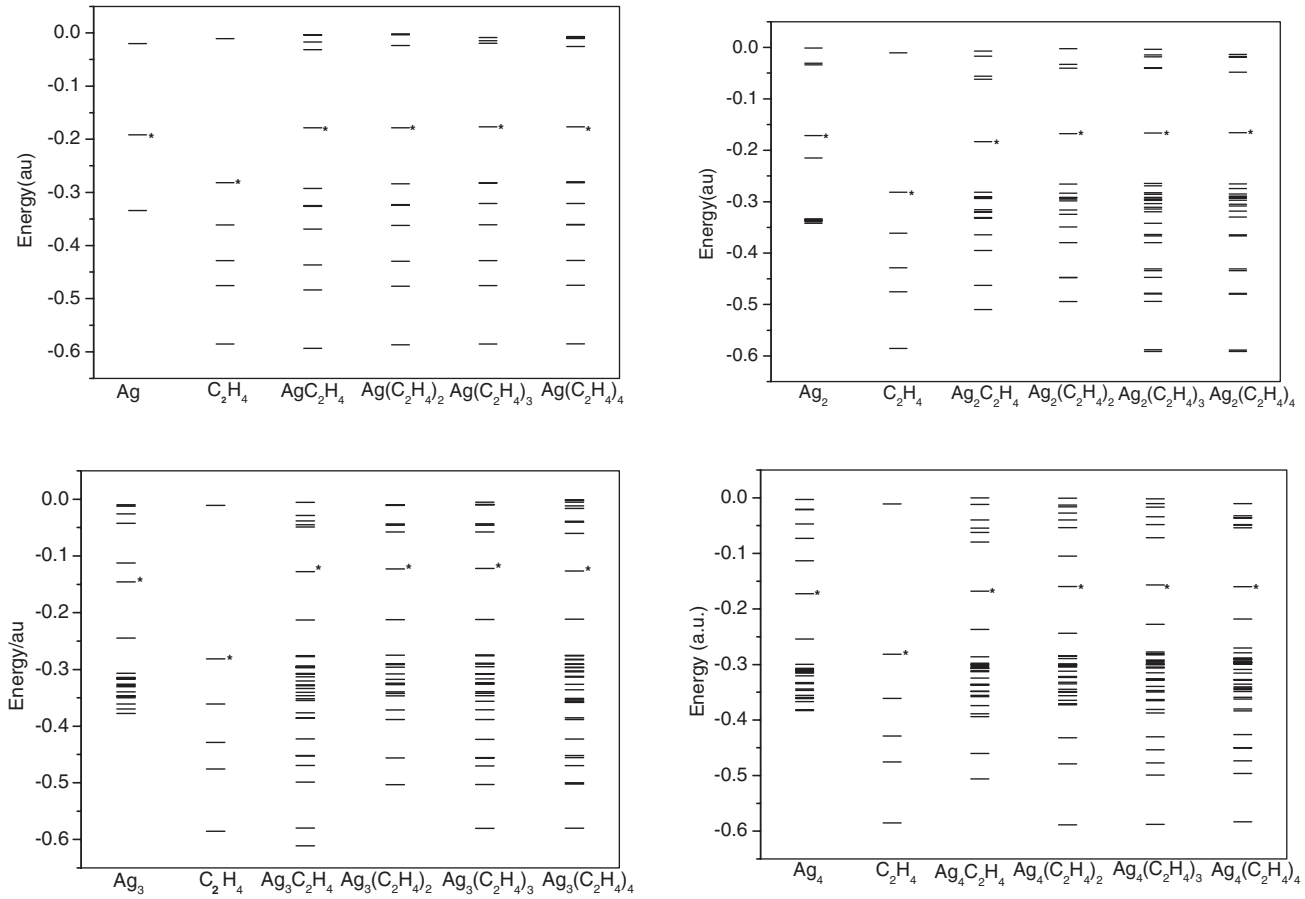

Figure 7. Energy levels (ranging from −0.6 to zero in atomic units) of molecular orbitals for the corresponding neutral species of the Ag_n^+ (n = 1–4), C_2H_4, and the most stable equilibrium isomer of $Ag_n(C_2H_4)_m^+$ (n = 1–4, m = 1–4). HOMOs are indicated with asterisks.

molecules in some degenerate isomers of $Ag_n(C_2H_4)_m^+$ complexes, as discussed above, lie between 10–80 cm^{-1} but mainly near 30 cm^{-1}. The harmonic frequencies corresponding to the C=C stretch are listed in Table 1. The calculated C=C stretching vibration frequency of the free ethylene molecule is 1648.7 cm^{-1}, in good agreement with the experimental value (1623 cm^{-1} with 6–15 cm^{-1} uncertainty).[61] The C=C double bond is weakened due to significant charge transfer to the silver cluster, so the C=C stretching vibrational frequencies are about 30–70 cm^{-1} lower than that of the free ethylene molecule. The C=C stretching vibrational frequencies in $Ag(C_2H_4)_m^+$ have the most rapid increase with increasing m from 1 to 4, compared to those of $Ag_n(C_2H_4)_m^+$ (n = 2–4), which indicates that the binding between the silver cluster moiety and the original ethylene molecules is more sensitive to the addition of other ethylene molecules in $Ag(C_2H_4)_m^+$. This conclusion is consistent with the previous one that significant ion–molecule interaction exists only between the adjacent atomic metal ion and ligand molecule. Generally, the absolute difference of the C=C stretching vibration frequency between that in the free ethylene molecule and those in $Ag(C_2H_4)_m^+$ is a little larger than that between the free ethylene molecule and $Ag_n(C_2H_4)_m^+$ (n = 2–4), which is also consistent with the previous deduction that the distribution of the positive charge when the metal cluster grows larger is disadvantageous for the metal–ligand interaction.

Binding energies

The incremental binding energy of C_2H_4 to a complex $Ag_n(C_2H_4)_{m-1}^+$, $\Delta E(Ag_n(C_2H_4)_m^+)$, is defined as:

$$\Delta E(Ag_n(C_2H_4)_m^+) = D_e(Ag_n(C_2H_4)_m^+) - D_e(Ag_n(C_2H_4)_{m-1}^+)$$

and is drawn as a function of m in Fig. 6(D).

Both $\Delta E(Ag(C_2H_4)_m^+)$ and $\Delta E(Ag_2(C_2H_4)_m^+)$ show very rapid decreases as m increases from 1 to 3, while this decrease becomes rather smaller as m increases from 3 to 4, which indicates that the addition of the fourth ethylene molecule weakens the binding between the silver cluster and the original three ethylene molecules. $\Delta E(Ag_3(C_2H_4)_m^+)$ and $\Delta E(Ag_4(C_2H_4)_m^+)$ seem to show rather smooth decreases when m increases from 1 to 4, except that a rapid decrease occurs for $\Delta E(Ag_3(C_2H_4)_4^+)$. Generally, $\Delta E(Ag_n(C_2H_4)_4^+)$ begins to approach zero.

Energy levels and VIPs

Energy levels (ranging from −0.6 to zero in atomic units) of molecular orbitals for the corresponding neutral species of the silver cluster cations Ag_n^+ (n = 1–4), C_2H_4, and the most stable equilibrium isomers of $Ag_n(C_2H_4)_m^+$ (n = 1–4, m = 1–4), are shown in Fig. 7. The highest occupied molecular orbitals (HOMOs), the second highest occupied molecular orbitals (SHOMOs), or the third highest occupied

RCM

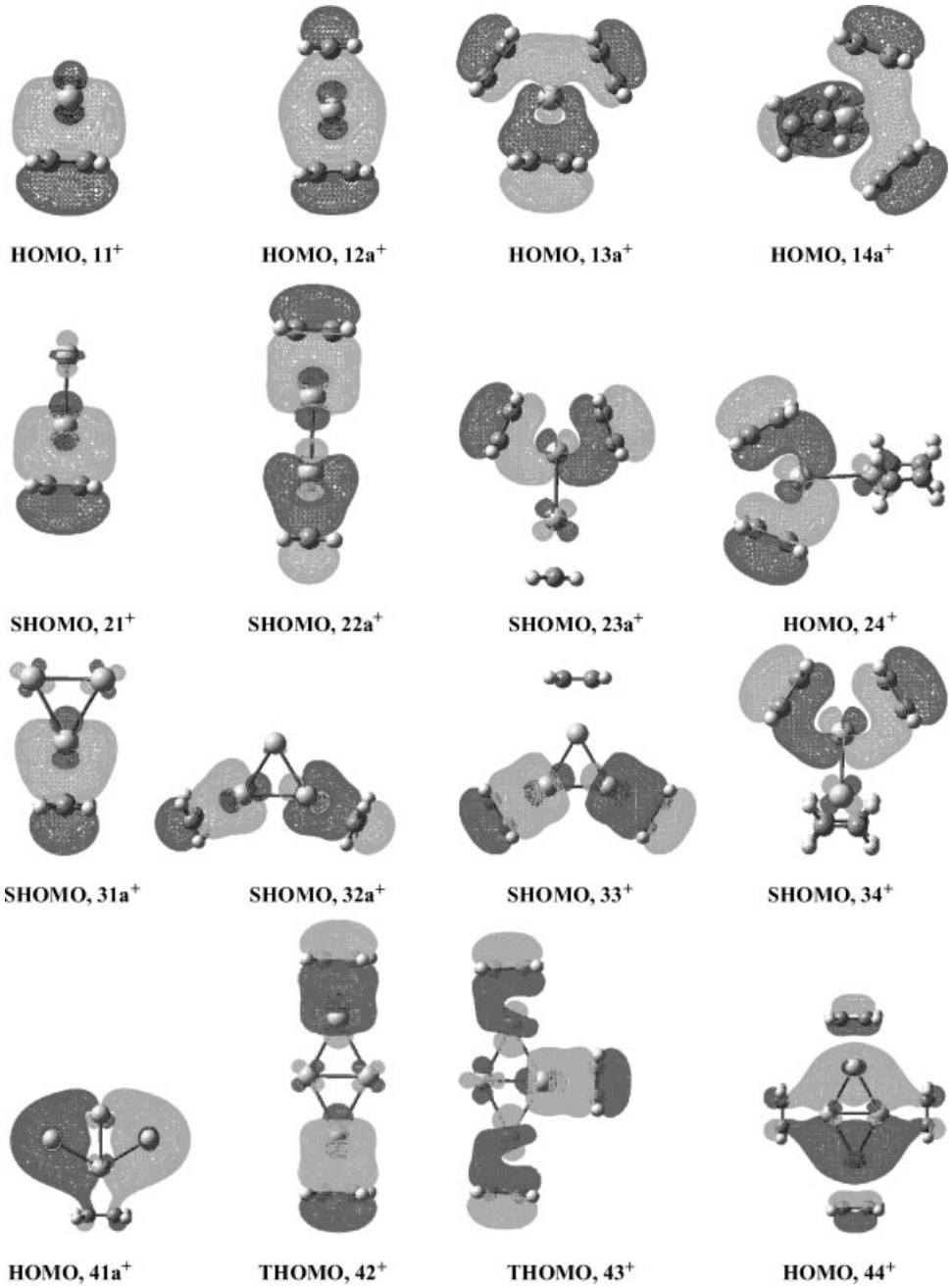

Figure 8. HOMOs, SHOMOs, or THOMOs for the most stable equilibrium isomer of $Ag_n(C_2H_4)_m^+$ (n = 1–4, m = 1–4). The notation nmx$^+$ used to represent $Ag_n(C_2H_4)_m^+$ is the same as that used in Fig. 4.

molecular orbitals (THOMOs) for the most stable equilibrium isomer of $Ag_n(C_2H_4)_m^+$ (n = 1–4, m = 1–4) are shown in Fig. 8. If the interaction between the carbon and silver orbitals is not observed in the HOMOs, then the SHOMOs or THOMOs are provided in Fig. 8 instead of HOMOs. It is obvious that the HOMO energy levels of $Ag_n(C_2H_4)_m$ (n = 1–4, m = 1–4) are around those of the corresponding Ag_n (n = 1–4) species, but considerably higher than that of C_2H_4.

By comparing the atomic charges for the neutral and corresponding cationic $Ag_n(C_2H_4)_m$ (n = 1–4, m = 1–4) species, part of the electron charge removed from the silver cluster moiety Ag_n (n = 1–4) upon ionization of the neutral $Ag_n(C_2H_4)_m$ (n = 1–4, m = 1–4) species are summarized in Table 2. For a given value of n, i.e., a fixed silver cluster moiety in $Ag_n(C_2H_4)_m$, less and less electron charge is removed from the silver cluster moiety as m increases from 1 to 4; on the other hand, for a given value of m, i.e., a fixed number of ethylene molecules in $Ag_n(C_2H_4)_m$, more and more charge is removed from the silver cluster moiety when n increases from 1 to 4. The loss of an electron upon ionization of the complex will take place to a larger degree from the silver cluster moiety rather than the ethylene molecule(s) of the complex, in agreement with the fact that the VIP of the silver cluster moiety is substantially smaller than that of the ethylene molecule. However, it should be noted that the electron charge removed from the silver cluster moiety in $Ag(C_2H_4)_3$ is much smaller than 0.5 and those in $Ag(C_2H_4)_4$ and $Ag_2(C_2H_4)_4$ are near zero, which indicates that electron charges are mainly removed from the ethylene molecules upon the ionization of these three complexes.

Table 2. Part of electron charge removed from the silver cluster moiety Ag_n (n = 1–4) upon ionization of the neutral $Ag_n(C_2H_4)_m$ (n = 1–4, m = 1–4) corresponding to the most stable equilibrium isomers of $Ag_n(C_2H_4)_m^+$ (n = 1–4, m = 1–4)

	Ag_n			
$(C_2H_4)_m$	1	2	3	4
1	0.650	0.861	1.125	0.933
2	0.552	0.714	0.788	0.775
3	0.245	0.458	0.624	0.663
4	0.005	0.084	0.526	0.502

Another characteristic for the energy levels is that the HOMO energy levels of $Ag_n(C_2H_4)_m$ (n = 1–4, m = 1–4) species are generally a little higher (0–1 eV) than those of the corresponding Ag_n (n = 1–4) species. Accordingly, the VIPs of the neutral $Ag_n(C_2H_4)_m$ (n = 1–4, m = 1–4) species are generally a little lower than those of the corresponding Ag_n (n = 1–4) species, which is consistent with the prediction of a electrostatic model[62,63] and the experimental photoionization results.[32] This electrostatic model predicts that the adsorption of non-polar species onto metal clusters will lead to an decrease in IP due to the stabilizing effect of the charge-induced dipole interaction. The VIPs of the most stable equilibrium isomers of $Ag_n(C_2H_4)_m$ (n = 1–2, m = 1–4), shown in Table 1, are generally much larger than 6.4 eV, which is the reason that Koretsky and Knickelbein[32] did not observe these complexes in their TOF spectrum of $Ag_n(C_2H_4)_m$ complexes obtained by photoionization of the corresponding neutral species at 193 nm ($h\nu = 6.42$ eV). VIPs of $Ag_n(C_2H_4)_m$ (n = 3–4, m = 1–3) calculated here are in very good agreement with the corresponding experimental values.[32] From the above analysis of VIPs, we believe that the most stable equilibrium isomers of $Ag_n(C_2H_4)_m$ (n = 1–4, m = 1–4) found here are the dominant, if not exclusive, structures of the species generated under the experimental conditions.

It can be easily observed in all the HOMOs in Fig. 8 that there is considerable interaction between the carbon and silver orbitals.

CONCLUSIONS

The interaction of silver cluster cations Ag_n^+ with ethylene to form $Ag_n(C_2H_4)_m^+$ complexes has been studied using reflectron time-of-flight mass spectrometry coupled with extensive theoretical investigations at the DFT level. The predominant reaction channel observed under experimental vaporization-expansion condition was association of ethylene, $Ag_n(C_2H_4)_m^+$ (n = 1–3, m = 1–6). For a given value of n, $Ag_n(C_2H_4)_m^+$ had first an increasing and then a decreasing intensity distribution as m increased, with the maximum at m = 3 or 4; this characteristic did not change with the concentration of ethylene in the mixed gas, the stagnation pressure of the mixed gas, or the size of Ag_n^+.

The Ag atom in the most stable equilibrium isomers of $Ag_n(C_2H_4)_m^+$ prefers to lie right above (perpendicular to) the ethylene molecule plane, which corresponds to the π-bonded adsorption of the ethylene molecule on the bulk silver surface. Effective ion–molecule interaction only exists between the adjacent Ag^+ and ethylene. Ethylene deforms from D_{2h} symmetry in the free molecule into C_{2v} in $Ag_n(C_2H_4)_m^+$ complexes, i.e., a substantial rehybridization occurs for the ethylene molecule upon adsorption, with four hydrogen atoms pushed back to form a plane on the side of the C=C double bond and considerable elongation of the C=C double bond. The adsorption of additional non-polar ethylene molecules onto the silver clusters leads to a monotonic decrease of VIPs of $Ag_n(C_2H_4)_m$ (n = 1–4, m = 1–4) in comparison with those of the bare silver clusters. The loss of an electron upon ionization of the neutral $Ag_n(C_2H_4)_m$ (n = 1–4, m = 1–4) takes place to a larger degree from the silver cluster moiety.

Acknowledgements

We gratefully acknowledge the support of the National Natural Science Foundation of China under Grant 20203020. Some of the calculations were done on the Supercomputing Environment of Computer Network, Information Center, Chinese Academy of Sciences. We are thankful to Dr. Guoliang Li and Tujin Shi for helpful discussions.

REFERENCES

1. Geurts P, Van Der Avoird A. *Surf. Sci*. 1981; **102**: 185.
2. Geurts P, Van Der Avoird A. *Surf. Sci*. 1981; **103**: 416.
3. Hermann K, Witko M. *Surf. Sci*. 1995; **337**: 205.
4. Dewar MJS. *Bull. Soc. Chim. Fr*. 1951; **18**: C79.
5. Chatt J, Duncanson LA. *J. Chem. Soc*. 1953; 2939.
6. King DA, Woodruff DP. In *Fundamental Studies of Heterogeneous Catalysis*. Elsevier: Amsterdam, 1984.
7. Friend CM, Xu X. *Annu. Rev. Phys. Chem*. 1991; **42**: 251.
8. Somorjai GA. In *Introduction to Surface Science and Catalysis*. John Wiley: New York, 1994.
9. Dietz TG, Duncan MA, Powers DE, Smalley RE. *J. Chem. Phys*. 1981; **74**: 6511.
10. Song L, El-Sayed MA. *J. Phys. Chem*. 1990; **94**: 7907.
11. Jiao CQ, Freiser BS. *J. Phys. Chem*. 1995; **99**: 10723.
12. Parent DC, Anderson SL. *Chem. Rev*. 1992; **92**: 1541.
13. Knickelbein MB, *Philosoph. Mag. B* 1999; **79**: 1379.
14. Tang JC, Feng XS, Shen JF, Fujikawa T, Okazawa T. *Phy. Rev. B* 1991; **44**: 13018.
15. Haslett TL, Brosnick KA, Moskovits M. *J. Chem. Phys*. 1998; **108**: 3453.
16. Yang DS, Zgierski MZ, Hackett PA. *J. Chem. Phys*. 1998; **108**: 3591.
17. Riley SJ, Noncryst J. *Solids* 1996; **205/207**: 781.
18. Upton TH, Goddard WA III, Melius CF. *J. Vac. Sci. Technol*. 1979; **16**: 531.
19. Messmer RP, Tucker CW Jr, Johnson KH. *Chem. Phys. Lett*. 1975; **36**: 423.
20. Fan HJ, Liu CW, Liao MS. *Chem. Phys. Lett*. 1997; **273**: 353.
21. Basch H. *J. Chem. Phys*. 1972; **56**: 441.
22. Reed AE, Weinstock RB, Weinhold F. *J. Chem. Phys*. 1985; **83**: 735.
23. Hosoya H, Nagakura S. *Bull. Chem. Soc. Jpn*. 1964; **37**: 249.
24. Carter EA, Goddard WA. *Surf. Sci*. 1989; **209**: 243.
25. Boussard Per JE, Siegbahn Per EM, Svensson M. *Chem. Phys. Lett*. 1994; **231**: 337.
26. Ito M, Suzaka W. *Surf. Sci*. 1977; **62**: 308.
27. Manojlovic-Muir L, Muir KW, Ibers JA. *Discuss. Faraday Soc*. 1969; **47**: 84.
28. Cunningham GL Jr, Boyd AW, Meyers RJ, Gwinn WD, LeVan WI. *J. Chem. Phys*. 1951; **19**: 676.
29. Petersson GA, Bennett A, Tensfeldt TG, Al-Laham MA, Shirley WA, Mantzaris J. *J. Chem. Phys*. 1988; **89**: 2193.
30. Backx C, de Groot CPM. *Surf. Sci*. 1982; **115**: 382.

31. Tang JC, Shen JF, Chen LB. *Surf. Sci. Lett*. 1991; **244**: L125.
32. Koretsky GM, Knickelbein MB. *J. Chem. Phys*. 1997; **107**: 10555.
33. Tian ZX, Xing XP, Tang ZC. *Rapid Commun. Mass Spectrom*. 2003; **17**: 17.
34. Frisch MJ, *et al. Gaussian 98, Revision A.9*. Gaussian, Inc.: Pittsburgh PA, 1998.
35. Chan WT, Fournier R. *Chem. Phys. Lett*. 1999; **315**: 257.
36. Hertwig RH, Koch W, Schröder D, Schwarz H, Hrušák J, Schwerdtfeger P. *J. Phys. Chem*. 1996; **100**: 12253.
37. Aroca RF, Clavijo RE, Halls MD, Schlegel HB. *J. Phys. Chem. A* 2000; **104**: 9500.
38. Kim CK, Kim JW, Kim HS, Kang YS, Li HG, Kim CK. *J. Comput. Chem*. 2001; **22**: 827.
39. Wu K, Chen X, Snijders JG, Sa R, Lin C, Zhuang B. *J. Crystal Growth* 2002; **237/239**: 663.
40. Kickelbick G, Schubert U. *Inorg. Chim. Acta* 1997; **262**: 61.
41. Howard JA, Preston KF, Mile B. *J. Am. Chem. Soc*. 1981; **103**: 6226.
42. Salian U, Srinivis S, Jellinek J. *Chem. Phys. Lett*. 2001; **345**: 312.
43. Bonacic-Koutecky V, Pittner J, Boiron M, Fantucci P. *J. Chem. Phys*. 1999; **110**: 3876.
44. Santamaria R, Kaplan IG, Novaro O. *Chem. Phys. Lett*. 1994; **218**: 395.
45. Backx C, de Groot CPM. *Surf. Sci*. 1982; **115**: 382.
46. Arvanitis D, Baberschke K, Wenzel L, Dobler U. *Phys. Rev. Lett*. 1986; **57**: 3175.
47. Solomon JL, Madix RJ, Stohr J. *J. Chem. Phys*. 1990; **93**: 8379.
48. Hay PJ, Wadt WR. *J. Chem. Phys*. 1985; **82**: 284.
49. Hay PJ, Wadt WR. *J. Chem. Phys*. 1985; **82**: 299.
50. Bonacic-Koutecky V, Fantucci P, Koutecky P. *Chem Rev*. 1991; **91**: 1035.
51. Poteau R, Heully JL, Spiegelmann F. *Z. Phys. D* 1997; **40**: 479.
52. Franzreb K, Wucher A, Oechsner H. *Z. Phys. D* 1992; **22**: 517.
53. Buckner SW, Gord JR, Freiser BS. *Z. Phys. D* 1990; **17**: 51.
54. Martin JML, Taylor PR. *Chem. Phys. Lett*. 1996; **248**: 336.
55. Ohno K, Okamura K, Yamakado H, Hoshino S, Takami T, Yamauchi M. *J. Phys. Chem*. 1995; **99**: 14247.
56. Guo BC, Castleman AW. *Chem. Phys. Lett*. 1991; **181**: 16.
57. Ffischer K, Jonas K, Misbach P, Stabba R, Wilke G. *Angew Chem*. 1973; **85**: 1002.
58. Basch H, Newton MD, Moskowitz JW. *J. Chem. Phys*. 1978; **69**: 584.
59. Willey KF, Cheng PY, Bishop MB, Duncan MA. *J. Am. Chem. Soc*. 1991; **113**: 4721.
60. Winstead CB, Paukstis SJ, Gole JC. *Chem. Phys. Lett*. 1995; **237**: 81.
61. Shimanouchi T. In *Tables of Molecular Vibrational Frequencies*, Consolidated Volume I, National Bureau of Standards, 1972.
62. Knickelbein MB, Menezes WJC. *Chem. Phys. Lett*. 1991; **184**: 433.
63. Knickelbein MB, Menezes WJC. *J. Phys. Chem*. 1992; **96**: 6611.